Thermal Decomposition of Mechanoactivated Technical Fluorocarbon Materials

VALENTIN N. MITKIN, PETR P. SEMYANNIKOV and ALEXANDER A. GALITSKY

Institute of Inorganic Chemistry, Siberian Branch of the Russian Academy of Sciences,
Pr. Lavrentyeva 3, Novosibirsk 630090 (Russia)

E-mail: *mit@che.nsk.su*

(Received May 15, 2001; in revised form February 11, 2002)

Abstract

The features of the processes of thermal decomposition of mechanoactivated technical fluorocarbon materials (FCM-MA) of substoichiometric and superstoichiometric composition in vacuum and inert media have been studied at 250–600 °C by methods of thermal analysis and high-temperature mass spectrometry. The mechanoactivation of FCM has been shown to intensify the processes of hydrolysis and pyrohydrolysis of C–F bonds by a chemisorbed moisture to form hydrogen fluoride and low-molecular carbon oxyfluorides, that results in decrease of the thermal stability of these FCMs by 20–70 °C and simplifies their mass-spectra in comparison to non-activated samples at the expense of reduction of the yield of the high-molecular products of thermolysis of fluorocarbon nanoblocks. The likely pattern of the FCM-MA thermofragmentation is suggested. The mechanoactivation of materials is shown to reduce the properties dissimilarities for technical FCMs of a different nature.

INTRODUCTION

It is well known that the fluorocarbon materials offer promise as the energy carriers for lithium current sources (LCCS). Using them as the base, the most power-intensive electrochemical systems are created, and since 1980 the fluorocarbon-lithium CCS of BR brand mark have no competitors in the market as to electrical capacity and safety. The technical fluorocarbon materials (FCM) of the general formula CF_x are used in these LCCS, where $x = 0.5–0.92$ (fluorinated petroleum coke or graphite fluoride) [1]. The new superstoichiometric fluorocarbon materials with the higher fluorine content [2, 3] of the general formula $CF_{1.1-1.33}$ were developed in the late 1980s in Russia. Their application to LCCS made possible the next stage in CF_x – Li electrochemical system capacity increase and allowed to create the new generation of lithium current sources of effective energy intensity up to 600–650 mA h/g by fluorocarbon cathode material [4], which is 30–40 % higher than the best parameters of Japan manufacturer fluorocarbon LCCS. This effect was achieved, in particular, not only by virtue of application of the new fluorocarbon materials with the increased fluorine content [5], but also by use of mechanoactivation to increase the discharge current density in the cathodes of fluorocarbon-lithium current sources [6, 7].

There is always the contact of FCM with an atmospheric moisture in the course of cathode matter manufacturing for LCCS. Besides, vacuum thermotreatment is used. The purpose of the present work is to study the composition of the gas phase formed in the course of thermolysis of technical fluorocarbon materials, which were subjected to preliminary mechanoactivation (FCM-MA), by methods of high-temperature mass spectrometry (HTMS) and thermal analysis (TA).

EXPERIMENTAL

Initial fluorocarbon materials

Industrial technical FCMs of two types were used as investigation objects: superstoichiometric fluorocarbon materials of FS and FT brand marks (polycarbonofluorides) of composition $CF_{1.25-1.33}$ [8] manufactured by Angarsky Electrolysis Chemical Plant and substoichiometric fluorocarbons of composition CF_{1-x}, including powder material of ITG-01 brand mark [9] produced by Kirovo-Tchepetsky Chemical Plant, together with laboratory sample of grey-coloured graphite fluoride (GF) of composition $CF_{0.88}$ obtained by fluorination of 40–70 mm fraction of the cleaned natural graphite according to the well known pattern [1, 10] at 565–590 °C.

All FCMs were subjected to mechanoactivation with the use of planetary-friction APF-8 unit at 80 *g* acceleration of striking bodies for 3–5 min (the batches of 100–150 g were used) [6]. The chemical analysis of mechanoactivated FCMs for the fluorine content, humidity [11], free acidity (HF), and for the presence of trace metal contaminants [12] was executed by procedures described in [8, 9] (Table 1). Besides, the IR spectroscopic study of all FCMs and GF was carried out.

Taking into account that samples of FCM, used in the present work, had various shelf lives (from 3 to 12 months) from the moment of their preparation, to be able to compare them, all the samples, prior to study, were processed with fluorine-argon mixture (1 : 1) at the temperature of 430–470 °C to remove the traces of moisture.

The equipment

Thermoanalytic investigations have been made at computerized derivatograph Q1000 (MOM, Hungary) by the use of covered platinum microfirepots. Derivatograms have been registered at helium boost (the flow rate of 5–8 l/min) and the heating rate of 5–10 °C / min. The batches of FCM-MA were in the range of 90–150 mg. The deciphering of derivatograms was carried out by the original author's program TGMA-Pro. As a reference substance, α-Al_2O_3 of "extra pure" qualification has been used as well as, warmed in the helium current up to constant weight, granulated carbon material (fraction of 50–200 μm) of Technosorb brand mark. Temperature of characteristic sites of effects on DTA and DTG was determined following the tangent method [13].

The IR spectra were taken through tableting FCM powder batches of 2–4 mg in the carefully dried KBr with the use of IR-85 Fourier-IR spectrometer (Bruker) following the procedure [14].

The study of mass-spectra of mechanoactivated FCM has been performed using MI-1201 and MKh-1310 mass spectrometers, tailored to

TABLE 1

Data of chemical analysis of mechanoactivated samples of graphite fluoride and industrial FCMs

FCM sample	Colour	Content of F, % mass	F : C atomic ratio	Content of HF, % mass	Content of the sum of metals, % mass*	Content of moisture, % mass
FT-MA	The white dense powder with grey shade	66.6±0.6	1.25±0.04	0.07±0.01	0.09	0.13± 0.02
FS-MA	The same	65.2±0.2	1.18±0.03	0.12±0.01	0.17	0.17± 0.02
ITG-MA	Dark-grey dense powder	57.7±0.2	0.87±0.03	0.06±0.005	0.47	0.11± 0.01
FG-MA	Dark-grey powder with glint	58.7±0.2	0.89±0.02	0.012±0.005	0.07	n/d

*Spectral analysis data (S_r = 0.2).

suit the high-temperature experiments. Nickel high-temperature Knudsen molecular guns were used with an outer diameter of 2.5 mm, and effusion aperture of 0.1–0.3 mm. The temperature range comprised 25–700 °C. The mass spectra of gas phase of FCM thermolysis products were obtained by method of the electronic impact of electron energy of 35 eV and the ionization chamber temperature of 250–590 °C. The weighted samples were in the range of 3–5 mg. The experimental procedure is described in [15].

RESULTS AND DISCUSSION

Thermoanalytic features of FCM-MA decomposition processes

Derivatograms of FCM-MA thermolysis processes in the inert media (He, heating rate of 20 °C/min) are given in the Fig. 1. The behavior of FCM-MA on heating is rather similar in appearance to earlier investigated processes of thermolysis of the raw FCMs [7]. The form of DTA curves shows that, in the course of heating of all FCM-MA (except for ITG-MA), there were no noticeable thermal effects detected down to temperature T_2, and on TG curves, in the area of relatively low temperatures ($T_0 = 150–450$ °C), only smooth and small mass changes are registered (Table 2).

We used the following symbols on FCM-MA thermolysis derivatograms: T_0 – temperature of pyrohydrolysis, T_1 – the beginning of the first stage of thermolysis, T_2 – the beginning of the main stage of thermolysis, T_m – adjusted temperature of the maximal development of thermolysis process (with the maximal velocity of the mass loss), T_f – temperature of termination of all the processes of FCM thermolysis, T_{m_2} – temperature of the maximal development of the processes of the small mass loss, upon the completion of the main stage of thermolysis, Δm_0 –mass loss up to temperature T_0, Δm_1 – mass loss up to T_1, and Δm_2 – mass loss up to T_2 of thermolysis (see also Table 2).

The analysis of the Fig. 1 demonstrates that the sharp one-step decrease of samples weight, accompanied by intensive exoeffects on DTA curves, is exhibited only at the temperatures of about 500–700 °C. The form of these exoeffects depends on the FCM-MA type, the rather simple single-component form being exhibited only in thermolysis of FG-MA (see Fig. 1, *a*), while the exoeffects in ITG-MA, as well as in FS-MA, FT-MA thermolysis, are of rather complex three or even four-component form (see Fig. 1, *b*, *c*).

As opposed to thermoanalytic data for all FCM-MA, the derivatogram of ITG-MA thermolysis (see Fig. 1, *b*) shows that, in the field of temperatures of 170–470 °C, some process of heat release proceeds in this material, which is not connected with the mass change. It turned out also that FS-MA and FT-MA derivatograms (see Fig. 1, *c*) are practically identical in their form and differ only in the temperature parameters and values of mass loss.

The character of TG and DTA curves makes it possible to conclude that in the course of ITG-MA, FS-MA, and FT-MA thermolysis, the

TABLE 2

Comparison of derivatograms data of FCM and FCM-MA thermolysis in the atmosphere of helium (heating rate of 20 °C/min, Δm_i are normalized to the total mass loss)

FCM sample	Δm_0, %	Δm_1, %	T_1, °C	T_2–T_{m1}–T_f, °C	Δm_2, %	Δm_3, %
FS	0.6–0.8	6.5	>500	635–670–685	23.1	96.5
FS-MA	0.7–1.2	12.2	420	610–635–650	50.0	92.2
FT	0.3	3.0	540	640–680–720	25.0	95.0
FT-MA	0.6–0.8	20.4	360	620–657–700	55.9	92.8
ITG	0.3–0.4	2.6	>400	588–665–678	21.0	94.4
ITG-MA	0.7–0.9	7.4	360	545–648–680	39.2	73.4
FG	0.05–0.1	1.3	–	645–687–695	15.8	97.1
FG-MA	0.1–0.2	6.9	530	630–654–652	27.8	94.2

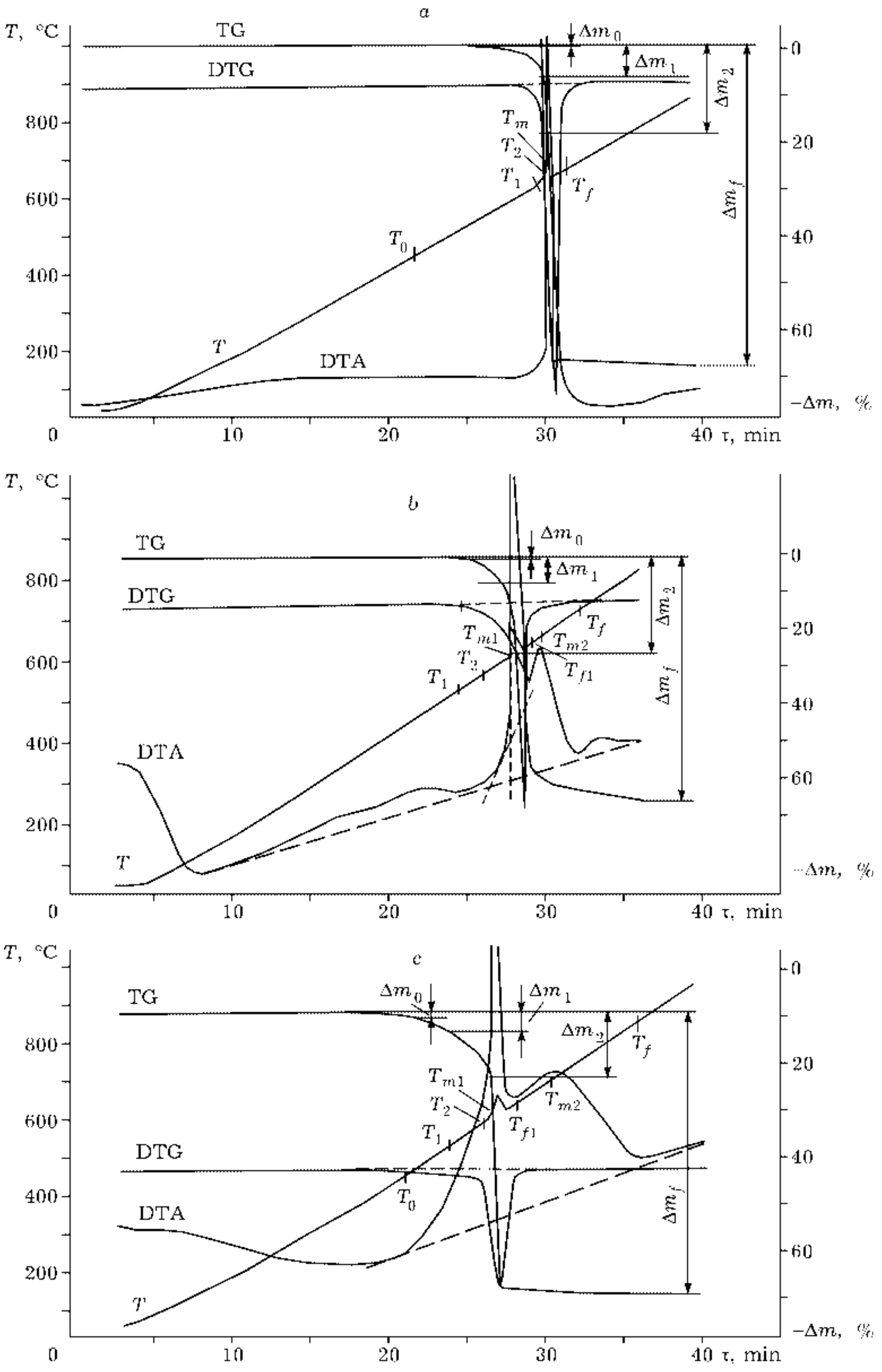

Fig. 1. Typical derivatograms of the thermolysis processes of FG-MA (*a*), ITG-MA (*b*), FS-MA and FT-MA (*c*) in inert media (the flow rate of helium 5 l/min, covered platinum microfirepot, 20 °C/min).

consecutive processes, proceeding in essentially different temperature ranges and sharply distinct in velocity and power parameters, take place: the slow decrease of weight with no significant thermal effects (except for ITG-MA, where an insignificant heat release occurs) at T_0–T_1 at the first stage, fast two-stage exothermal explosion-like thermolysis in the range of T_1–T_2 (the beginning and the development of the previous, rather slow stage of thermolysis), the main explosion-like thermolysis T_2–T_m–T_{f1} and terminating stage T_{m2}–T_{f2} with the small mass loss, upon the completion of all stages of thermolysis.

The residue of thermolysis of all types of FCM-MA appears to contain only amorphous carbon (so-called residual carbon [1]). With reference to data of Table 2, it can be seen that the loss of weight of a sample manifests itself distinctly on TG curves, starting from temperatures $T_1 < T_2 < T_{m1}$. It is found that T_0 and T_1, for all types of FCM-MA, are approximately 50–150 °C less than for non-activated FCMs [16]. These temperatures are almost the same as the top limit of the temperature range of 150–350 °C for the processes of removal of sorption moisture and other volatile products from porous substances [17], though, in the case, they are a little bit higher (280–400 °C). The temperatures of intensive decomposition beginning (T_2), of maximal development (T_{m_1}) and of the end of the main exoeffect of thermolysis processes (T_{f_1}) for FCM-MA, which were determined from the method of tangents crossing with the linear component of temperature growth plot [14] at the rates of heating of 5–20 °C/min, turned out to be 20–30 °C below than those for non-activated FCMs at the same heating rates (see Table 2) [16, 18]. They increase in the following succession of relative kinetic thermal stability of mechanoactivated FCM: FT-MA > FS-MA > ITG-MA > FG-MA.

Lines of relative kinetic stability of FCM-MA and non-activated FCMs to thermolysis determined on relative velocity of processes at the temperatures T_2–T_m–T_{f1}, expressed in terms of Δm_1 and Δm_2 (at equal heating rates), are equal both for activated, and non-activated FCMs. The main distinction between these types of FCM, on evidence of DTA and TG (see Fig. 1, Table 2), lies in the fact that Δm_1 and Δm_2 at the comparable threshold temperatures of comparison, T_2, for FCM-MA is several times greater than for initial FCMs. In particular, intensity of the main process of thermolysis (as to parameter Δm_2) for FG-MA and ITG-MA is 1.7–1.8 times higher, and for FS-MA and FT-MA, 2.0–2.2 times higher than for non-activated FCMs.

Even greater difference is observed in the velocities of the beginning of the processes at T_1: for FT-MA and FS-MA $\Delta_{\mathrm{m}1}$ is 2–7 times, and for FG-MA and ITG-MA is 3–5 times higher, compared with initial samples.

As T_1 and T_2, for FCM-MA, are shifted by 17–40 °C towards low temperatures (see Table 2, [18]) as compared to non-activated samples, in view of above-mentioned, it is possible to make an unambiguous conclusion that FCM-MA are more reactive than non-activated FCMs. On evidence of TA (compare T_1 and T_2, Δ_{m_1} and Δ_{m_2}), FT and FS types of FCM are most sensitive to mechanoactivation, ITG-01 and FG are least sensitive.

We reported earlier that, on evidence of FTIR spectroscopy, EPR and electrochemical methods, the mechanical impact under power-intensive planetary-friction unit conditions with acceleration of striking bodies of 40–200 *g*, results in emergence of various kinds of damages and defects in internal macro-, micro-, and nanostructures of FCM, which will cause an increase of the concentrations of unpaired spins, a decrease of specific resistance and size of CDR (coherent dispersion regions) of nanocrystallites, an increase of an acidity of materials, change of the thermal stability [4–8, 10–12, 14, 18], an increase of their bulk density, and also a substantial increase of the discharge current density of these FCMs used as cathode materials in primary lithium CCS of CF_x – Li electrochemical system.

The main consequence of this complex change of microgeometry and superficial energy of FCM-MA particles, in our opinion, is the increase of FCM reactivity as a whole.

The gas phase products of thermolysis of FCM-MA

Mass-spectra of gas phase products of two stages of thermolysis of FCM-MA are pre-

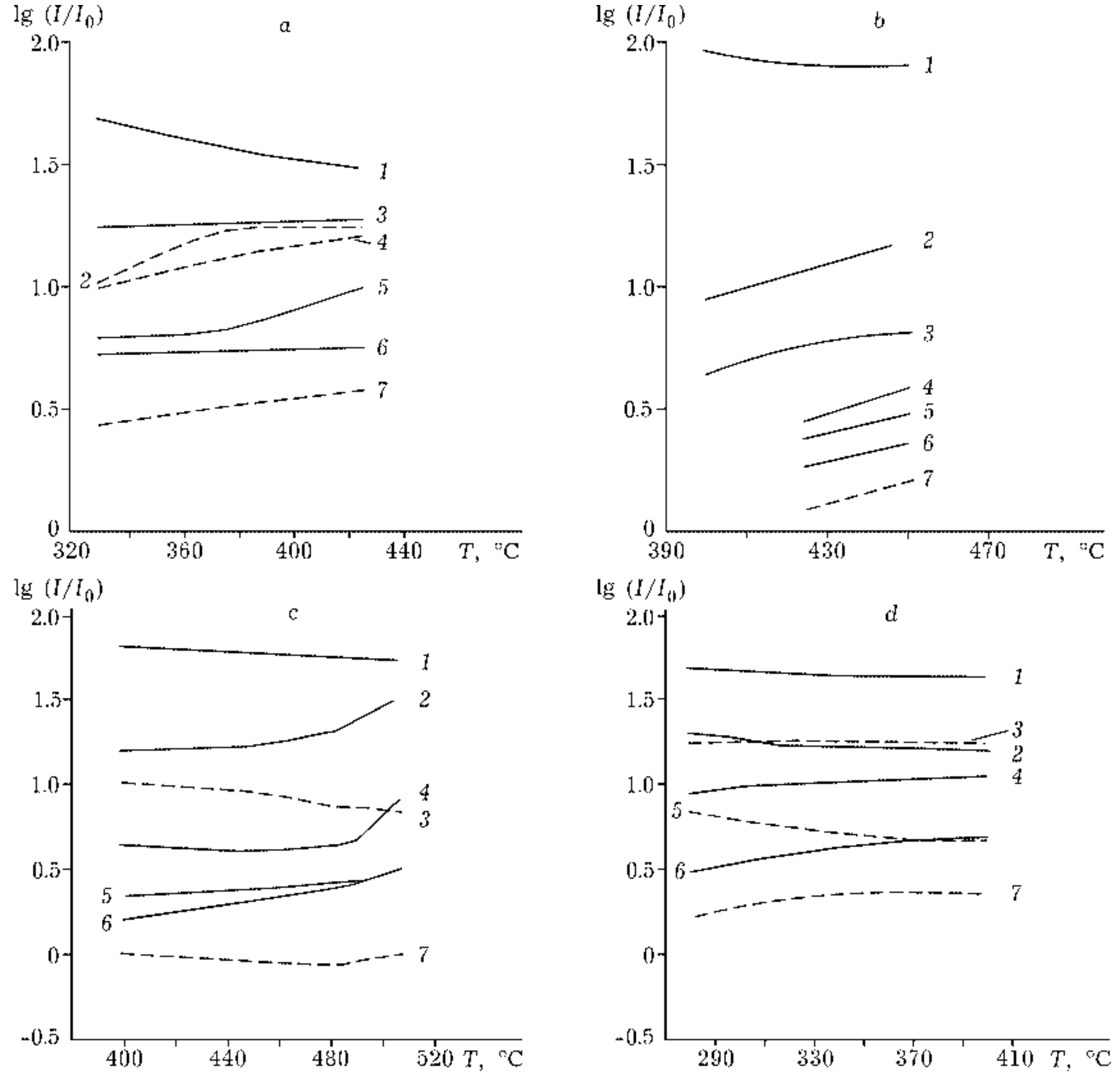

Fig. 2. Temperature dynamics in the emergence of C_iF_x fragments in the mass-spectra of FS-MA (*a*), FT-MA (*b*), ITG-MA (*c*) and FG-MA (*d*).

sented in Figs. 2, 3. The characteristics of the obtained mass-spectra are given in Tables 3, 4. The analysis of these data shows that the main distinctive feature of the thermal behaviour of FCM-MA is the emergence of the distinct mass-spectra even at 140–350 °C, *i. e.* under the conditions, when distinct effects (except for ITG-MA) are not detected yet on DTA curves, but the weight loss (up to 6 % for ITG-MA, see Fig. 1) is already quite noticeable on TG curves. This range of temperatures is 100–150 °C lower than the one we reported earlier for mass-spectra of gas phase of thermolysis of non-activated FCMs [16, 18–20]. Another feature of FCM-MA thermolysis is the sharp difference in composition of gas phase from that of initial FCMs both for the slow initial stages of exothermal thermolysis (T_0–T_1 at 470–540 °C), and for the fast exothermal stage at the maximal development of processes (T_2–T_m–T_f at 556–660 °C).

There are no standard, for FCM, fragments of $C_iF_x^+$ fluorocarbons in the gas phase of thermolysis of mechanoactivated fluorocarbon materials at 140–350 °C, but there exist the large number of compounds involving oxygen and hydrogen, including H_2O, hydrogen fluoride, together with various carbon oxyfluorides. In particular, the intensive peaks of COF_3^+ ions and their splinters (m/z = 85, 66, 47) are observed in mass-spectra of all samples of FCM-MA, shown in Tables 3, 4 and on Fig. 3.

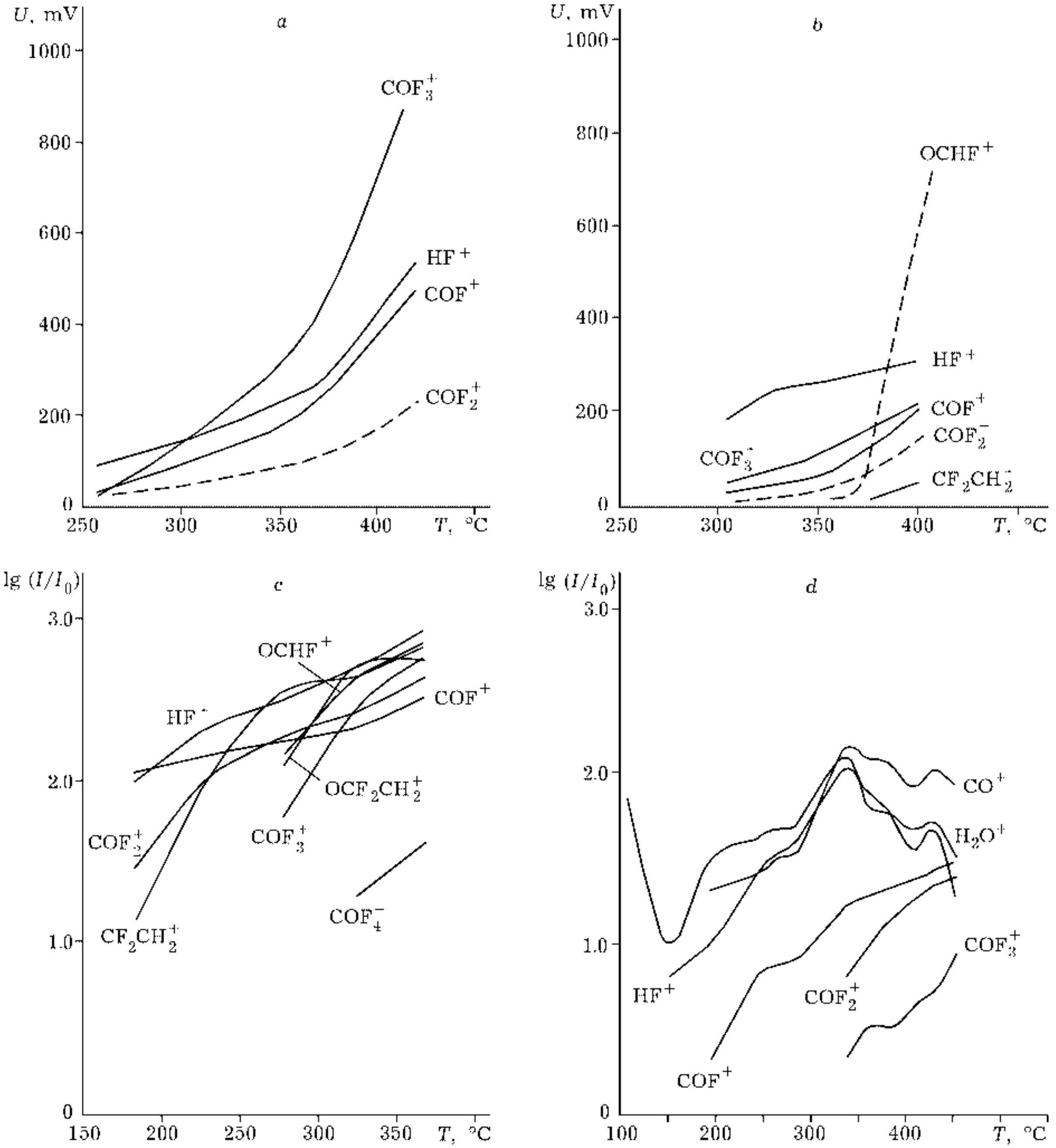

Fig. 3. Temperature dynamics in the emergence of O- and H-bearing fragments in the mass-spectra of FS-MA (*a*), FT-MA (*b*), ITG-MA (*c*) and FG-MA (*d*).

Here, the quantity of carbon atoms in these fluorine- and oxygen-bearing splinters varies from 1 to 3. The growth of relative intensity of all peaks with temperature growth is observed, including formation of HF, of oxyfluorides COF_3^+ and their splinters (see Fig. 3). The maximum of peaks intensity of hydrogen and oxygen-containing fragments is exhibited at various temperatures even by different batches of the same sample, which is testimony to heterogeneity of distribution of their sources in FCM matrixes. It was shown in works [14, 18–20] that such basic source is the moisture, and the moisture fixation in FCM has a number of specific features, which were established by methods of chemical analysis and IR spectroscopy.

The analysis of the form of Fourier-IR spectra for the initial and mechanoactivated FCMs given in Fig. 4, shows that all the spectra, along

TABLE 3

The intensity of ionic peaks in the gas phase mass-spectra of the products of FCM-MA thermolysis at 420–530 °C, %

Ionic peak	ITG-MA (420)	FG-MA (450)	FS-MA (530)	FS-MA (430)	FT-MA (430)	FT-MA (530)
H_2O^+	9.2	0.1	–	>1.0	>1.0	–
HF^+	96.0	8.0	11.0	13.0	27.6	7.1
CO^+	8.2	0.5	–	<0.1	–	–
CF^+		15.2			27.9	31.2
COF^+	57.7	6.3	4.0	12.0	25.9	21.6
$CFOH^+$	96.1	–	1.0	–	–	0.5
CF_2^+	30.7	17.2	16.0	2.0	19.7	21.6
$C_2F_2H_2^+$	100.0	–	2.0	7.0		
COF_2^+	73.0	5.1	4.0	5.0	25.9	21.6
$C_2F_2H_2O^+$	94.2	–	–	–	–	–
CF_3^+	40.3	100	100	100	100	100
COF_3^+	100	92	>100 (explosion)	26.0	295	160
$C_2F_3^+$		81	–	–	49.1	51.2
$C_2F_3OH^+$	67.3	10.2	–	–	–	–
$C_3F_3^+$		2.8	–	–	32.1	13.8
$C_2F_4^+$	34.6	13.8	27.2	30.0	43.1	32.4
$C_3F_3H_2O^+$	30.7	–	–	–	5.7	2.8
$C_2F_5^+$	76.9	2.8	39.7	45.0	9.8	7.3
$C_3F_5^+$	81.0	5.6	19.2	41.0	27.4	21.5
$C_4F_5^+$	9.6	1.6	3.6	4.2	6.2	6.2
$C_3F_6^+$	4.1	1.0	2.2	6.1	10.3	6.8
$C_4F_6^+$	10.6	1.5	6.1	8.0	7.7	8.6
$C_5F_5^+$		1.0	1.7	4.6	16.6	7.4
$C_3F_7^+$	30.8	1.0	8.0	40.0	10.3	3.2
$C_4F_7^+$	50.0	2.0	9.2	41.0	6.2	4.8
$C_6F_6^+$	8.6	0.4	–	–	–	–
$C_5F_7^+$	13.4	1.2	3.1	–	–	6.6
$C_6F_7^+$	7.7	1.7	–	–	–	6.6
$C_5F_8^+$	3.9	2.3	2.8	–	5.9	4.7
$C_4F_9^+$	8.6	0.7	–	–	2.6	1.1
$C_5F_9^+$	28.8	1.1	–	–	0.4	0.4
$C_6F_9^+$	9.8	2.3	3.8		6.8	6.4
$C_6F_{10}^+$	4.1	0.8	4.4		–	1.8
$C_8F_9^+$	2.4	0.8	1.4		–	1.4
$C_7F_{10}^+$	1.9	0.4	0.5		–	0.7
$C_7F_{11}^+$	2.4	0.7	0.4		–	1.6
$C_9F_{10}^+$	1.3	0.3	0.9		–	0.3
$C_9F_{11}^+$	2.4	0.6	0.2		–	1.0
$C_{10}F_{11}^+$	2.1	0.3	0.3		–	0.3
$C_8F_{13}^+$	5.7	0.1	0.1		–	0.2
$C_{11}F_{12}^+$	1.1	0.1	0.06		–	0.04
$C_{10}F_{13}^+$	1.1	0.5	0.03		–	0.4
$C_{11}F_{13}^+$	0.8	0.3	0.03		–	0.2
$C_{10}F_{14}^+$	0.3	0.2	0.01		–	–
$C_{12}F_{13}^+$	0.4	0.3			–	–
$C_{13}F_{13}^+$	0.6	0.2			–	–
$C_{12}F_{15}^+$	0.4	0.2			–	–
$C_{12}F_{16}^+$		0.1				

TABLE 4

Yield of the gas phase products in thermolysis of mechanoactivated fluorocarbon materials FCMs at 420–530 °C, %

Characteristics of ionic peaks	ITG-MA (420)	FS-MA		FT-MA		FG-MA (450)
		530	430	430	530	
Even/odd ratio.	0.96	0.62	0.61	0.53	0.57	0.24
Peaks total without HF, $C_1OF_x^+$ and water, arb. units	1103.8	360.2	382.3	393.2	359.9	374.9
Peaks total including H_2O+HF, arb. units	1209.0	371.2	382.3	851.5	886.0	383.0
Moisture*	0.76	<0.1	<0.25	1.34	0.15	<0.03
HF*	7.94	2.96	3.40	3.24	1.21	2.09
$\Sigma C_1OF_x^{+}$ *	27.52	29.36	11.24	37.66	30.85	2.70
	(stable spectrum)	(3–5 % after 10 min)	(stable spectrum)	(stable spectrum)	(3–5 % after 10 min)	(stable spectrum)
CO^+	0.68	–	<0.25	12.91	6.80	0.13
$C_1F_x^{+}$ *	5.87	31.24	26.68	17.33	25.96	34.57
$\Sigma C_2F_xO_y^{+}$ *	13.36	–	–	–	–	2.66
$\Sigma C_2F_x^{+}$ *	9.22	18.02	19.62	11.97	15.53	25.48
$\Sigma C_2F_2H_2^+$ (CO_2HF^+?)*	8.27	0.54	1.83	–	–	–
$\Sigma C_3F_x^{+}$ *	9.59	7.92	22.78	10.50	9.49	2.72
$\Sigma C_3OF_x^{+}$ *	2.54	–	–	–	–	–
$\Sigma C_yOF_x^+ + C_2F_2H_2^+$	51.69	29.90	13.07	49.31	39.01	5.36
		(3–5 % after 10 min)			(3–5 % after 10 min)	
$\Sigma C_4F_x^{+}$ *	6.52	5.09	13.91	3.88	4.13	1.51
$\Sigma C_5F_x^{+}$ *	3.81	1.86	–	2.43	2.79	1.20
$\Sigma C_6F_x^{+}$ *	2.16	2.21	–	–	1.58	1.36
$\Sigma C_{1-6}F_x^+$	37.17	64.48, 93.5	82.99	46.11	59.48, 95.5	65.84
		(after 10 min)			(after 10 min)	
$\Sigma C_{7-12}F_x^+$	1.91	1.06	–			1.38

*The data for the first 3–5 min of thermolysis in the cases, when the mass-spectra are not stable with time. At 430 °C, the spectra get stable after 10 min during the registration.

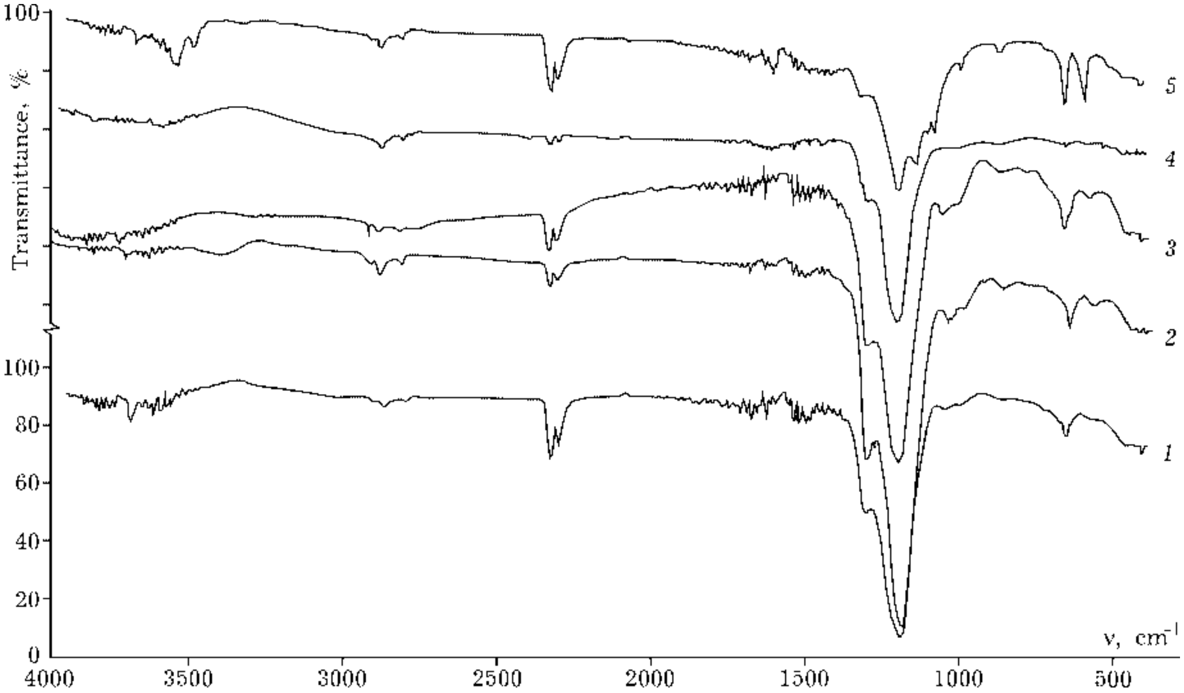

Fig. 4. Fourier-IR spectra of FS-MA (*1*), FT (*2*), FT-MA (*3*), ITG-01 (*4*) and ITG-MA (*5*).

with absorption bands characteristic of stretching vibrations ν_3 for C–F sp^3 bonds in CF and CF_2 groups in the field of frequencies of 1230 and 1350 cm^{-1}, contain carbonyl band (>C=O) at 1560 cm^{-1} as well as bands of absorption at 3750, 2350 and ~1600–1650 cm^{-1}. Last mentioned three bands qualify as stretching and deformation vibrations of CO_2 and H_2O molecules in FS-MA, ITG-MA and FT-MA, these bands having the resolved rotary structure, that is characteristic of IR spectra of molecules in the gas phase. On the basis of these data we made a conclusion that the water involved in FCM, is rather strongly bonded, *i. e.* it is chemisorbed, fixed by hydrogen bonds at O-donating centres (of >C=O type and even of COOH one), and also in defects of fluorocarbon materials nanostructures.

In our works [14, 16, 18, 20], on the strength of a totality of physical methods data, including IR spectroscopy, the suggestion has been made that H_2O is present in FCM initially as the residual moisture, which existed even in source carbon materials prior to their fluorination and obtaining of FCM from them, which is still held in the form of water molecules, isolated in the nanostructure “cells” of FCM. Such isolated molecules of H_2O can be removed only in destruction of “cellular” structures.

According to data of Table 1, both initial, and mechanoactivated FCMs contain some quantity of moisture and also are of rather high acidity. In this connection it is important to emphasize that the effect of short-term mechanoactivation of FCM manifests itself as the same increase of an acidity of these materials that is observed on their long storage. This effect marked by us in [18, 20] and assigned to the result of a slow hydrolysis of C–F bonds by the moisture in the source (non-activated) FCMs, is in the same way accompanied in FCM-MA by formation of HF, which is one of the main products of gas phase at moderate temperatures (140–200 °C, see Fig. 3).

Hence it follows that mechanoactivation of the FCM, first of all, sharply accelerates the process of C–F bonds hydrolysis, proceeding on the “contact” surface of FCM nanostructures with the large amount of water molecules existing there, and, instead of C–F sp^3 bonds, C–OH sp^3 bonds are produced, hydrogen fluoride being released in the process, which is further held by hydrogen bonds on any O-donating centers. Besides, doubtlessly, the mechanochemical process of moisture interaction with FCM occurs on shock impact, which is accompanied by accumulation of not only HF, but also low-molecular products $C_{2-5}F_xO_yH_z$ and

$C_xF_yO_z$. Some part of these low-molecular products, which do not have chemical affinity to oxygen or hydrogen, for example perfluorocarbons C_2-C_5, will be lost in short time because of the volatility of $C_{2-5}F_{4-10}$ and will not be registered in mass-spectra. It is likely also that in mechanoactivation of FCM-MA, no significant amount of liquid perfluorocarbons of C_6-C_{16} type can be generated, otherwise these products would be registered in the mass-spectra at 100–300 °C.

Thus, adsorptive, or, more precisely, chemisorbed on O-donating centers, water should be first of all considered as the source of hydrogen- and oxygen-bearing fragments in FCM-MA mass-spectra at 140–350 °C.

It is necessary to note such an important circumstance that H and O bearing splinters (HF and various $C_{1-3}F_{1-3}O_y$ and even $C_{1-2}F_xO_yH_z$) make their appearance and dominate in mass-spectra of FCM-MA even at rather low temperatures (190–300 °C), the fluorocarbon splinters $C_iF_x^+$ being still absent in this range (see Fig. 3), and the mass-spectra of non-activated FCMs with the same H- and O- splinters being yet not so distinctly pronounced [18, 20].

Moisture content in FCM-MA samples (see Table 1) ranges up to about 0.1–0.2 %, that is much enough. An estimation of intensity of O- and H-containing fragments of ITG-MA and FT-MA, which are liberated at 140–350 °C (see Fig. 3), shows that one water molecule in gas phase accounts for no less than five-six various molecular fragments $C_{1-2}F_xO_yH_z$ and $C_{1-2}F_xO_y$, together with HF. The percent of HF, on evidence of Table 4, at temperature increase up to 420–430 °C during the first 3–5 min of spectra registration (before stabilization of mass-spectra) exceeds the percent of H_2O in gas phase already by 1–2 order of magnitude, but is approximately an order lower than percent of $C_{1-2}F_xO_yH_z$ and $C_{1-2}F_xO_y$ fragments. If the content of water, HF and fragments of $C_{1-2}F_xO_yH_z$ type are compared, then, in gas phase of ITG-MA thermolysis (see Table 4), at higher temperatures (350–430 °C), the ratio of H_2O, HF, $C_1F_xO_y$ (taking the average values – COF_2) and $C_2F_yO_z$ (taking the average values – $C_2O_2F_2$) will comprise ~0.04 : ~0.4 : ~0.4 : ~0.1, *i. e.* one water molecule, upon the reactions completion, in gas phase, will account for more than 20 various molecules, splinters of interaction of H- and O-containing molecules with FCM surface. With such comparison however, the question arises of an estimation of the quantitative ratio between C, H, O, F splinters of thermolysis and initial water in FCM.

To estimate the molar ratio of thermolysis products and initial moisture, we used a reported method of stoichiography [21], which allows, on evidence of mass-spectrometry data, to restore stoichiometric coefficients of elements in complex substances of unknown composition. The results of calculation of relative molar intensity of C, H, O, F splinters in mass-spectra for all FCM-MA at 420–450 °C are given in Table 5, the calculation of molar and mass ratios of the total of C, H, O, F splinters and H_2O molecules being performed within the framework of a hypothesis, according to which the initial atoms of hydrogen in FCM-MA are represented only by water. The stoichiometric quantity of oxygen determined on mass-spectra, was compared to the quantity of hydrogen, which allowed to make a conclusion about the presence or absence of its excess in various FCM-MA, and also to suggest, what is the nature of H- and O-bearing impurities available in these materials.

Results of stoichiographic calculations presented in Table 5, demonstrate that the molar ratio of intensity of C, H, O, F-splinters and initial water comprises 6.00, 17.01, 6.75 and 24.82 for ITG-MA, FG-MA, FS-MA and FT-MA, respectively. The ratio of the sum of atoms of initial water and atoms of oxygen (taken by one) in the same line comprises ~4.26, 0.28, 2.20 and 0.18, respectively. Let's note that the calculation of the molar ratios at 420–430 °C is in good agreement with an estimate of these ratios at lower temperatures (see Fig. 3).

It should be emphasized that experimentally obtained molar ratios of C, H, O, F products and initial H_2O in all cases exceed the limiting stoichiometry of gas phase in respect to water (3 : 1), which follows, for example, from the simplest equation of pyrohydrolysis of C–F bonds in a FCM of a conventional composition $CF_{1.0}$:

$$4CF_{1.0} + H_2O \rightarrow COF_2 + 2HF + 3C \qquad (1)$$

TABLE 5

Stoichiographic analysis of C, H, O, F products of the gas phase of FCM-MA thermolysis

Characteristic	ITG-MA (420)	FG-MA (450)	FS-MA (430)	FT-MA (430)
Molar intensity H/O in the fragments, rel. units:				
H_2O^+	1.022/0.511	0.012/0.006	0.112/0.056	0.112/0.056
HF^+	4.800/–	0.400/–	0.650/–	1.380/–
CO^+	–/0.293	–/0.018	–	–
COF^+	–/1.202	–/0.134	–/0.256	–/1.264
$CFOH^+$	2.002/2.002	–	–	–
$C_2F_2H_2^+$	3.125/–	–	0.219/–	–
COF_2^+	–/1.106	–/0.077	–/0.076	–/0.393
$C_2F_2H_2O^+$	2.356/1.178	–	–	–
COF_3^+	–/1.724	–/1.082	–/0.325	–/3.471
$C_2F_3OH^+$	0.687/0.687	0.122/0.122	–	–
$C_3F_3H_2O^+$	0.552/0.276	–	–	0.102/0.051
The total stoichiometric coefficient H/O	14.544/8.979	0.634/1.439	0.981/0.713	1.594/5.235
The H_2O/O ratio	7.272/1.707	0.317/1.122	0.490/0.223	0.797/4.438
	(4.258/1.0)	(0.283/1.0)	(2.197/1.0)	(0.180/1.0)
The total stoichiometric coefficient C/F	14.697/23.758	1.433/4.544	0.876/2.176	5.281/14.236
	+5.206*	+0.134*	+0.256*	+1.264*
Molar ratio C_{tot}/H_2O	2.02	2.26	1.79	6.63
Mass ratio C_{tot}/H_2O	1.34	1.51	1.19	4.42
Molar ratio F/C:				
with HF	3.12	5.16	4.40	4.35
without HF	2.60	4.73	3.21	3.93
Molar ratio F_{tot}/H_2O	3.98	14.75	4.96	18.19
Mass ratio F_{tot}/H_2O	4.20	15.54	5.24	19.20
Molar ratio $(C + F)_{tot}/H_2O$	6.00	17.01	6.75	24.82
Mass ratio $(C + F)_{tot}/H_2O$	5.54	17.05	6.43	23.42

*With the consideration of the additional fluorine to convert the ions to the neutral molecules.

Stoichiographic analysis allows to explain experimentally available evidence by the fact that do not nearly all the atoms of hydrogen and oxygen in FCM belong to chemisorbed water only, but the rather significant part of them exists in the form of superficial functional groups of >C=O and COOH type, involving O-donating atoms. This conclusion agrees very well with the data of IR spectra of these FCM-MA (see Fig. 4). Moreover, we can add conclusions of the work [14] by an assertion that the absorption bands, unidentified before, in the area of ~2800–2900 cm^{-1} (see Fig. 4) should be most likely qualified as characteristic vibrations of C–H bond in >CH(OH) and CH(O) groups.

If the relative molecular weights of water and mentioned $C_{1-2}F_xO_yH_z$ splinters are compared within the framework of molar and mass ratios given in Table 5, it can be deduced that, at these rather low temperatures and initial content of water of 0.10–0.15 %, rather significant mass loss of FCM-MA, up to 0.56–3.8 %, may take place. If, in addition, the fact is taken into account that HF and some O-donating residues might be held by hydrogen bonds on the surfaces of matrixes of partially fragmented FCM nanostructures and might further enter into the subsequent reactions of autocatalytic character, then this low-temperature mass loss may exceed several tens times the mass of initial water. It is likely that it is just these kinds of processes that occur at the initial stages of thermolysis (up to T_1) in ITG-MA, FT-MA and FS-MA matrixes, since it is just them that the maximal losses of volatile products up to the temperatures of 360–420 °C, from 7 up to 24 % of the batch weight (see Table 2), are characteristic of. Molecular oxygen can have here a separate role as well, which will be the case in point a little bit later.

The intensity of H- and O-containing splinters keeps on dominating at 420–450 °C and exceeds, by almost the order of magnitude, the intensity of already arising ones in mass-spectra of $C_iF_x^+$, that is quite evident on comparison of data of Tables 3 and 4. As a whole, the comparison of integrated intensities of oxyfluoride splinters $C_{1-3}OF_x$ in individual mass-spectra of FCM-MA gives the ground for the following conclusion: the beginning of thermolysis of all mechanoactivated FCM is connected to a large extent with formation of hydrogen fluoride and carbon oxyfluorides, which fraction in the initial period of thermolysis is especially great. The percent of $C_{1-3}OF_x$ in gas phase of thermolysis of FCM-MA changes in the following line: ITG-MA/420 (43.7 %), FS-MA/530 (30.3 %), FS-MA/430 (11.9 %), FT-MA/400 (7 %) and FG-MA/450 (6.9 %), that confirms the fact of the least sensitivity of graphite fluoride to mechanoactivation.

The greatest dissimilarities in composition of gas phase of thermolysis are exhibited by FS-MA at the end of the first and in the beginning of the second stage of thermolysis (430–530 °C), that is evident from the data of Fig. 2 and Tables 2, 3. The mass-spectrum of gas phase of thermolysis of FS-MA at 430 °C is rather simple in appearance and has its termination in the field of C_4F_x splinters, the oxyfluoride splinters being represented entirely by C_1OF_x particles with one carbon atom, the fraction of which in the total spectrum is almost 12 %. However, the picture changes abruptly on temperature increase up to 530 °C: thermolysis gets "explosion-like" character of oxyfluorides liberating and is accompanied by equally fast fall of intensity of COF_3^+ ionic peaks and of other oxyfluoride splinters, as well as of hydrogen fluoride. Within a few minutes, the content of C_1OF_x in gas phase is stabilized at the level of 20–35 %, HF – up to 3 % from total gas pressure. It is possible that the source of "explosive" production of COF_3^+ and even COF_4^+ (carbonylfluoridehypofluorite) is the molecular oxygen blocked by some "cells" of FS nanostructure during its synthesis. Upon "the oxyfluoride explosion" and isothermal exposure at 530 °C, the intensity of COF-containing splinters flattens slowly out on the stationary mode (2–5 %), and the pressure of liberated HF even at 530 °C keeps on remaining at the level of 1.2–3.4 % from total pressure of gas phase and, practically, does not depend on the further increase of temperature. Let's remind that the temperature of 530 °C for all FCM-MA is the temperature of the beginning (T_2), not the maximal development of thermolysis (T_{m1}), and, after the process stabilization, the main components of gas phase of thermolysis of FS-MA, as evident from mass-spectra, are no longer oxyfluorides, but the fragments of $C_iF_x^+$ fluorocarbons, and mass-spectra of gas phase of products of thermolysis become similar to such of the raw FCMs. This implies that the sources of oxygen and hydrogen in FCM-MA matrixes exist even at 530 °C.

This feature of thermal behaviour of mass-spectra of FS-MA in the field of temperatures T_1–T_2 (see Figs. 1, 2), probably, is connected with the fact that the molecules of oxygen or water, conceivably, connected with the superficial functional groups by means of hydrogen bonds, can be kept indefinitely long in nanostructures of this superstoichiometric FCM (of composition ~$CF_{1.2}$), formed by the layers of fluorocarbon grids of sp^3 carbon with not only regular C–F bonds, but also regular inner grid holes with internal CF_2 bonds available. In any case, the size of these holes (8–11 Å), on evidence of quantum-chemical calculations, of XPS C 1*s* spectra and scanning electron microscopy [7, 11, 22–24], is quite sufficient for encapsulation of O_2 or H_2O molecules. In this connection one can suggest that the mechanism of oxygen "dissolving" in FS and FS-MA matrixes does not differ essentially from the reported fact of high oxygen solubility in related perfluorocarbon sp^3 structures, which involve CF_2 and CF bonds (in perfluorodecalin and perfluoroindan) [1]. Sure enough, this question calls for supplemental research and calculations.

The mass-spectrum of ITG-MA at 420 °C is enriched by $C_{1-3}OF_x$ oxyfluorides to even greater degree than the spectrum of FS-MA and yet the "explosive" process is not observed, since the thermolysis of mechanotreated ITG-01 proceeds in a rather quiet and stable manner. In addition, ITG-MA mass-spectrum, as opposed to other mechanoactivated FCM, has in its structure the various carbon oxyfluorides with one, two and even three carbon atoms (see Tables 3, 4). As it is evident from Figs. 2 and 3, the ITG-MA mass-spectrum is the richest one by quantity of various splinters of thermolysis containing hydrogen and oxygen atoms, besides usual, for FCM and FCM-MA, fluorocarbon fragments.

According to data of Tables 3 and 4 and Fig. 2, the maximal values m/z of $C_iF_x^+$ splinters of FCM-MA differ from the raw FCMs and decrease in the following sequence: FG-MA > ITG-MA > FT-MA > FS-MA.

In addition, the natural reduction of $C_iF_x^+$ peaks intensity is exhibited by the same samples of FCM-MA, the order of particles being the same, starting from $i > 4$ and $x > 6$.

The intensity ratios of ionic peaks of splinters with even and odd number of carbon atoms were calculated in the same way as for raw FCMs. This value $\lambda = I_{\text{even}}/I_{\text{odd}}$ is an individual parameter for all types of the studied FCM-MA. At temperatures of the process beginning, characterized as the minimal temperatures of stable spectra production, the λ value is equal 0.96, 0.62, 0.53 and 0.24 for ITG-MA, FS-MA, FT-MA and FG-MA, respectively. For the raw FCMs, the λ values are different in the same line: 0.69, 0.49–0.51, 0.75 and 0.34 [20]. What this means is, in the course of mechanoactivation of the FCMs, the fraction of fragments with odd number of carbon atoms is essentially increased in splinters of the fragmentation, except for FCM of the FS and ITG type. Most likely, it is related to the character of distribution of the reaction centers in FCM matrixes, the formation of even and odd splinters getting almost equally probable for ITG-MA, and mechanoactivation of FG-typed FCM resulting in the four-fold prevalence of odd splinters. It is essential that such extreme characteristics are obtained only for substoichiometric FCMs distinguished by rather low specific surface (about 10 m^2/g for FG-MA and about 80 m^2/g for ITG-MA) in comparison to specific surface of FT-MA and FS-MA (360–600 m^2/g).

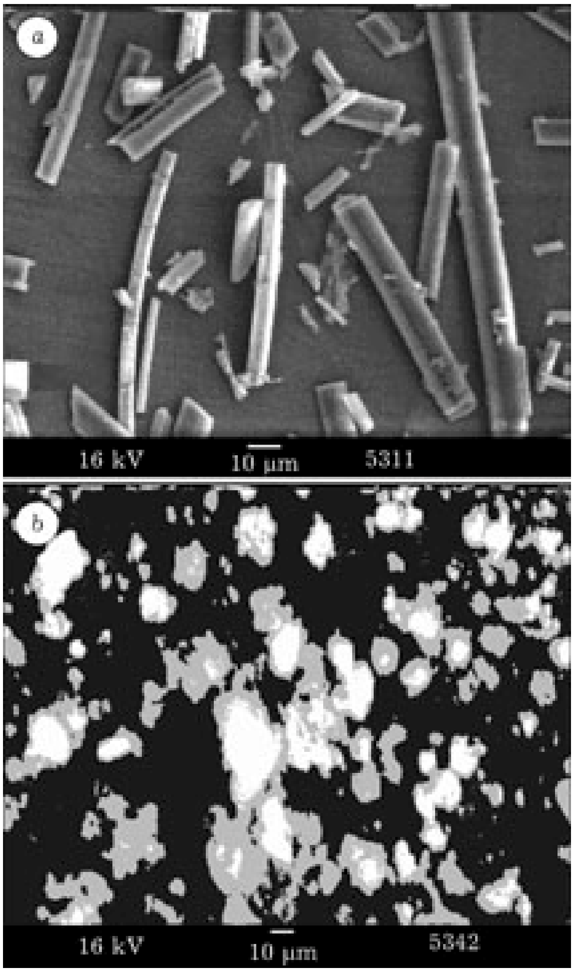

Fig. 5. Micrography of ITG-01 (*a*) and ITG-MA (*b*) particles (EMS Tesla).

As to dynamics of the emergence of $C_iF_x^+$ fluorocarbon splinters produced in thermolysis of FCM-MA (in a stationary mode) (see Fig. 2), it is also an individual characteristic. Common features for all mass-spectra of mechanoactivated materials are the several times increase of splinters intensity in the C_{1-6} range, and also some simplification of spectra at the expense of "tails" reduction for heavy weights. In particular, the heaviest $C_iF_x^+$ splinters, their peaks intensity being at the level of 0.1 %, were the fragments with number of atoms $C_i < 12$ for all types of FCM-MA, as opposed to the heaviest ions $C_{17}F_x^+$ characteristic of raw FCMs.

From analysis of data of Tables 3 and 4 and also from temperature dynamics of $C_iF_x^+$ splinters (see Fig. 2), the important conclusion can be drawn related to the form of spectra of gas phase of FCM-MA. The bulk of fragments is limited to the splinters of six carbon atoms as maximum, the main contribution being made by fragments of one, two and three carbon atoms (CF_3^+, $C_2F_3^+$, $C_2F_4^+$, $C_2F_5^+$), and CF_3^+ fragments contribution to the total intensity comprises 5.9, 27.5, 12.2 and 60.8 % for ITG-MA, FS-MA (430 °C), FT-MA and FG-MA, respectively. The total share of the contribution to the total intensity of fragments C_2 is, in the same line, as follows: 17.6, 20.0, 17.3 and 11.8 %, and the percent of C_{3-4} fragments is 22.4, 36.0, 39.4 and 14.6 %. This implies that the FG-MA fragmentation proceeds with predominant enrichment of gas phase by the most simple and light splinters with one – two carbon atoms. This is the manifestation of the essential dissimilarity of gas phase of FG-MA thermolysis and products of ITG-MA thermolysis, which are appreciably represented (almost 44 %) by oxyfluorides at the initial stages and the development of the thermolysis (at T_2–T_m), and approximately as much (~48 %) consist of tetrafluoromethane and of splinters from simple perfluoroalkenes and perfluoroalkanes $C_iF_x^+$, where $i = 2$–6.

As we noted in [7, 18, 20], the analysis of products of thermolysis gas phase for non-activated FG and ITG of substoichiometric composition (F/C < 1.0) shows rather close affinity in composition of thermolysis products of these FCMs as per splinters $C_{1-6}F_x$ at the temperatures of the maximal development of the process. However, from features of thermal behaviour of FCM-MA (especially ITG-MA and FG-MA) it follows that, of all FCMs, the graphite fluoride in the least susceptible to mechanoactivation impact. Such distinction in properties of substoichiometric fluorocarbons of close composition (ITG-01 – $CF_{0.92}$, FG – $CF_{0.83}$) suggests that the ITG-01 nanostructures are less stable against strong mechanical influence than layered structures of fluorinated graphite involving goffered grids of sp^3 carbon with an impurity of unfluorinated regions of sp^2 carbon. This is related to the features of the source carbon material nanostructure, which cross-linking fragments are most likely coaxial nanopipes of sp^2 carbon, which, namely, make up the basis for micro- and macrostructure of carbon filaments. During the fluorination and preparation of ITG-01 the filaments shape, as it is evident from Fig. 5, *a* is retained. We assume that the surface of such nanopipes, in the same way as in FG material, is formed by crimped C–F sp^3 bonds, but because of convolution of fluorographite planes in nanopipes, there should exist some strain inside them, which is absent in FG grids. In our opinion, the existence of such strain in the main cross-linking sp^3 fragments of ITG should cause some decrease of the temperature of the beginning of decomposition (T_2) and maximal development (T_{m1}) of thermolysis of ITG and ITG-MA type materials in comparison to FG, which is actually the case (see Fig. 1, Table 2).

In addition to the above-mentioned nanostructural factor, the macrostructural factor, morphology of particles of these FCMs has an impact on thermal behaviour of ITG-MA and FG-MA. It has been noted that during mechanoactivation of ITG-01 there is a significant destruction of the initial filamentous macroparticles of this FCM (the diameter of 3–8 μm, the length of 50–70 μm), and, on evidence of scanning electron microscopy (see Fig. 5, *b*), ITG-MA particles are produced, 0.3–3.5 μm in size, of nearly the spherical shape. The essential is that the destruction of the initial ITG-01 particles, to form such particles, occurs only under very strong mechanical impact (acceleration of striking bodies of the order of 40–80 *g*) and is unattainable, when crushing in usual ball mills. Let's notice that ITG-01 is available just through grinding of slices of a fluorinated fabric in the ball mills.

Mechanoactivation of graphite fluoride particles up to 200 μm in sizes, as it is evident from Fig. 6, results also in production of rather fine particles, basically 2–5 μm sized (though the particles up to 15 μm may also be met with), which, upon strike treatment, practically lose their characteristic graphite habitus. However, this external morphological change of FG-MA particles, supposedly, has a little effect on internal nanostructural level of this

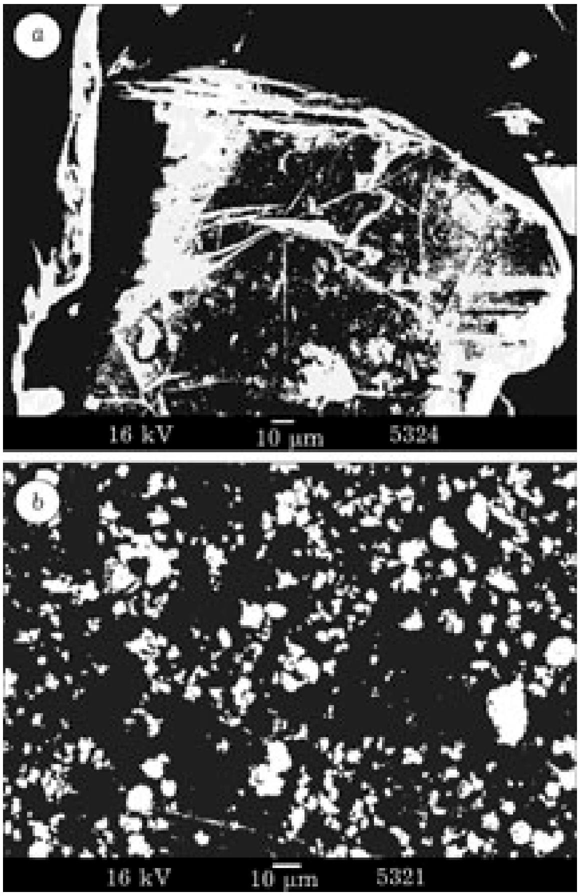

Fig. 6. Micrography of FG (*a*) and FG-MA (*b*) particles (EMS Tesla).

FCM structure, because the characteristic fluorographite reflexes on FG-MA X-ray patterns hardly change their half-width. This is confirmed by the fact that FG mechanoactivation does not result in drastic change of FG-MA thermal stability, on evidence of thermal analysis, and also does not give the so radical contribution of O- and H-involving splinters in gas phase products of the thermolysis beginning, as is characteristic of FS-MA and FT-MA types of FCM. Really, from data of Tables 3, 4 and Fig. 3 it follows that the contribution of COF_x and HF to the gas phase of the products of the beginning and development of thermolysis is minimal just for FG-MA, the fraction of such the splinters in the gas phase of this material thermolysis being less by more than an order of magnitude in comparison to other FCM-MA as well as to non-activated fluorocarbon materials [18, 20].

Interesting to note is that the most stable against mechanical damages in comparison to other FCM- MA are the internal nanoblocks of fractal nanostructures of a fluorocarbon of FT type based on sp^3 carbon, while the outer surfaces of these structures appear to be the most reactive in respect to moisture. At the first stage of FT-MA thermolysis, this shows up in the maximal concentration of oxyfluoride splinters, and yet at the second stage, the composition of the gas phase of thermolysis in respect to C_{1-6} splinters in the field of temperatures of the maximal development of the process undergoes hardly any serious changes (~80 % for FT-MA against ~89 % for the source FT [16, 18, 20]) *vs.* the raw material. This behaviour of FT-MA in thermolysis is in fairly good agreement with the fact that during the mechanoactivation of the given fluorocarbon, its microphysical and microchemical properties (the concentration of paramagnetic centers, the diffraction pictures, electric conductivity) are subject to the maximal changes on the surface of fractal nanostructures and to the minimal ones, in comparison to FCM of ITG and FS type, inside sp^3 fluorocarbon grids [4, 6]. Therefore, change of the sum of intensities of C_{1-6} splinters at the second stage of FT thermolysis, after the mechanoactivation, is moderate and is caused largely by formation of carbon oxyfluorides of the general formula COF_x.

The mechanism of formation of carbon oxyfluorides in mechanoactivated FCM thermolysis may be envisioned as a very simple one: we correlate it with the pyrohydrolysis of C–F bonds by moisture traces always available in FCM. It will suffice to mention that the mass fraction of a chemisorbed moisture in all FCMs, on evidence of an analysis, is usually in the range of about 0.05–0.25 % (sometimes 0.4–0.6 %), the tendency showing up in the maximal moisture accumulation by products of FS, ITG-01 and FT type. Therefore it is not surprising thing that all FCM after mechanotreatment completion have a sour smell, and a free fluoride-ion and H^+ in the form of HF may be found among the products by methods of the microchemical analysis [12].

The chemical pattern of a hydrolysis and pyrohydrolysis of C–F bonds in FCM and FCM-MA can be represented by simple primary reactions (2)–(7):


(2)

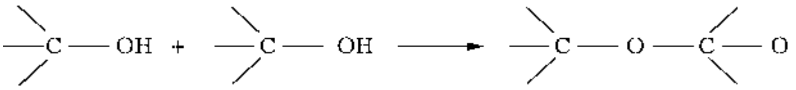
(3)

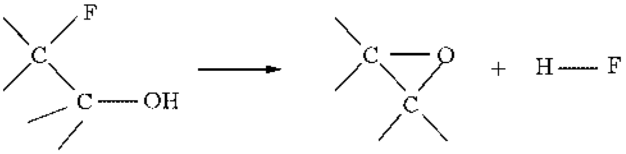
(4)

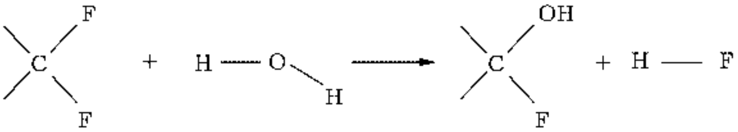
(5)

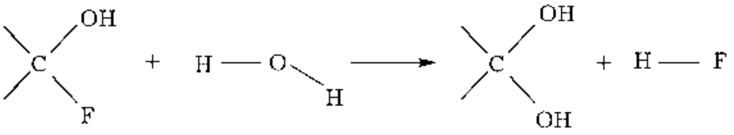
(6)

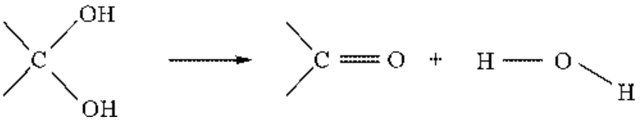
(7)

The consideration of the presented patterns of the hydrolysis and pyrohydrolysis demonstrates that the reactions (4) and (5) can result in production, at the next stage, of carbon oxyfluorides by breaking of two C–C bonds. In this connection the reality of the suggested mechanism is confirmed by the data of Fourier-IR spectroscopic investigation of non-activated and mechanoactivated FCM samples, which results are shown in the Fig. 4 and are described in detail by us in the work [14].

To monitor and quantitatively characterize hydrogen fluoride content in the source and mechanoactivated samples, we develop special analytic methods for a soluble fluoride ion and microacidity of a FCM [12] (see Table 1). The results of the analysis of FCM have shown that, in all cases, an increase of concentration of the free fluoride ion and acidity by 1.5–6 times in comparison with the source FCMs takes place after mechanoactivation, the acidity of FG-MA growing minimally, and the one of FS-MA maximally.

The thermal properties of FCM-MA samples also change appreciably. So, according to thermoanalytic data (see Fig. 1, Table 2), not only temperature intervals of decomposition of fluorocarbons in the atmosphere of helium and the general view of the mass loss curve depend on the preliminary mechanotreatment of samples, but so does the total mass loss of FCM-MA in the course of thermolysis (Δm_f to T_f). Here, the total mass loss Δm_f for non-activated FCM samples turned out to be greater in all cases (for the same heating rate, see Table 2) than for FCM-MA, the difference in the mass loss being more significant for substoichiometric FCMs (94.2 % for FG-MA against 97.1 % for FG and 73.4 % for ITG-MA against 94.4 % for ITG-01) than for superstoichiometric FS-MA and FT-MA materials, where the difference comprised 2.8–4.3 %. It means that the yield of "residual" carbon in the process of thermolysis of all FCM-MA is higher than in thermolysis of non-activated FCMs.

From the preceding it follows that the mechanical activation of FCM in the presence of a chemisorbed moisture results in changes both on the surface of FCM particles, and in the bulk of them. As the starting transformations begin just on the surface of the structural nanoblocks, it is possible to make a conclusion on predominantly superficial and rather profound changes.

An intensive mechanical impact on all types of FCM results in the severe damage of the outer regions of fluorocarbon grids at the nano- and microstructural level and, mostly important, in the amplification of the hydrolysis phenomena of C–F bonds by available moisture. The depth and intensity of the process should be related to the specific surface and morphology of FCM particles, to the duration of mechanical impact, and also to the moisture content in samples and places of its localization in nano- and microstructures of fluorocarbon particles. This is evidenced also by earlier described increase of volumetric and mass concentration of paramagnetic centers after mechanoactivation [6]. So, after mechanotreatment during 3 min in the planetary-friction APF-8 unit, the mass fraction of water-soluble fluoride ion in one of FS-MA samples has increased from 0.03 to 0.19 %, while ITG-01 and FT are characterized by a lower acidity in the same treatment conditions.

As the acidity grows in mechanotreatment, FCM-MA form the following line: FG-MA < ITG-MA < FT-MA < FS-MA – that is directly connected with the reactivity of these materials in relation to the moisture and with the order, in which their specific surface increases (8.5, 40, 280 and 420 m^2/g respectively for non-activated FG, ITG-01, FT and FS).

We consider that the nanostructural and morphological features of FCM structure are those principal factors, which, in combination with the existence of adsorption moisture in these samples at the first stage of the mechanoactivated samples thermolysis, predetermine the emergence of oxyfluoride splinters and HF in mass-spectra, and, at the final stage, simplify the character of fluorocarbons fragmentation and the composition of gas phase of the products of various FCMs thermolysis. Here, the determining factor is the increase of FCM reactivity after mechanoactivation completion, which, as a whole, results in reduction of the individual distinctions of particular FCMs and in substantial unification of their physicochemical properties.

It should be specially emphasized that the application of mechanoactivation appeared one of the principal decisions of the problem of sharp increase in reactivity of cathode matter around any types of FCM used in LCCS. In a number of our technical projects the new generation of fluorocarbon cathode composites has been created around the FCM-MA, which made it possible to raise the discharge current density in the CF_x – Li electrochemical system by almost the order of magnitude, to increase the efficiency of the cathode up to 96–99 %, the open-chain voltage and service voltage of the discharge by 10–15 % in comparison to Japanese analogues [6, 7, 23]. However, in testing of cathodes around FCM-MA it was established that such an important property, as the increased reactivity, is an advantage only in respect to the lithium anode and current source, and in respect to the moisture traces in non-aqueous electrolyte and in the porous cathode it may alter to essential drawback. It is shown that, moisture content being at the level of 0.02–0.05 % in finished LCCS with cathodes around FCM-MA, the microcorrosion processes begin to occur rather quickly, which are resulting in high self-discharge and the decrease of useful properties [25]. To counteract the high reactivity of FCM-MA in respect to moisture, to suppress the microcorrosion processes and create the LCCS with storage times of 5–12 years, we were forced to develop the special techniques for reduction of moisture content in cathodes, though it is the subject of the separate publication.

CONCLUSIONS

The processes of thermolysis of mechanoactivated technical fluorocarbon materials, FS and FT polycarbonofluorides of a superstoichiometric composition CF_{1+x} ($x = 0.18-0.25$), together with substoichiometric FCMs of the ITG-01 type and fluorinated graphite of composition CF_{1-x} ($x = 0.11-0.13$) have been studied by methods of HTMS and thermal analysis. It is shown that the main features of the thermal behaviour of mechanoactivated fluorocarbon materials, in comparison to non-activated ones, are the emergence of the pronounced mass-spectrum at much lower temperatures (100–150 °C less) and the sharp difference in composition of the gas phase at 400–530 °C containing, besides the fragments of $C_iF_x^+$ fluorocarbons, typical for FCM thermolysis, the large amount of compounds of carbon with fluorine, oxygen and hydrogen, including moisture, hydrogen fluoride, together with various carbon oxyfluorides. Under comparable conditions, the mass-spectra of the gas phase of thermolysis of mechanoactivated fluorocarbons are represented by the less quantity of $C_iF_x^+$ splinters, than for non-activated FCMs, the fraction of high-molecular fragments being decreased.

The mechanism of the emergence of hydrogen fluoride and carbon oxyfluorides in gas phase of the first stages of FCM-MA thermolysis connected with a pyrohydrolysis of C–F bonds by a chemisorbed moisture at 250–450 °C has been suggested and justified. The tendency of mechanoactivated FCM to the processes of hydrolysis and pyrohydrolysis changes in the following line: FT-MA > FS-MA > ITG-MA > FG-MA.

Mechanoactivated FCM can be used as the source substances for calibration of the scales of the high-temperature mass spectrometers.

REFERENCES

1 N. Watanabe, T. Nakajima, H. Touhara, Graphite Fluorides, Amsterdam *etc.*, Elsevier Science Publ., 1988, 263 p.

2 V. N. Mitkin, L. L. Gornostaev, S. V. Zemskov *et al.*, Pat. 2054375 RF, 1992.

3 I. G. Gurevich, O. S. Rabinovich, Yu. N. Kuznetsov *et al.*, Tez. dokl. 9 Vsesoyuz. simp. po khimii neorganicheskikh ftoridov, Nauka, Moscow, 1990, vol. 1, p. 20.

4 V. N. Mitkin, V. L. Afanasjev, A. I. Belosokhov *et al.*, 189 ECS Spring Meeting Abstr., Vol. 96-1, Los Angeles, California, May 5–10, 1996, Abstr. 46, p. 55.

5 V. N. Mitkin, L. L. Gornostaev, S. V. Filatov, Abstr. 14th Intern. Symp. on Fluorine Chemistry, Yokohama, 1994, p. 65.

6 V. N. Mitkin, I. I. Yakovlev, V. V. Rozhkov *et al.*, Pat. 2080288 RF, 1995.

7 V. N. Mitkin, Noveyshiye elektrodnye materialy dlya litievoy khimicheskoy energetiki, in F. A. Kuznetsov and V. V. Mukhin (Eds.), izd. OAO NZKhK, Novosibirsk. 2001.

8 V. N. Mitkin, L. M. Levchenko, P. S. Galkin *et al.*, TU 349735–0003–0353944–97, Novosibirsk *etc.*, 1997.

9 TU 16–88 ILEA.349735.003, Elektrougli *etc.*, 1988.

10 V. N. Mitkin, *Khimiya v Rossii*, 4 (2000) 3.

11 N. M. Gordik, N. M. Nederova, Opredeleniye vody i vodoroda v tverdykh materilakh, in V. N. Mitkin (Ed.), izd. OAO NZKhK, Novosibirsk. 2001.

12 V. N. Mitkin, L. M. Levchenko, T. N. Denisova *et al.*, Third APAM Topical Seminar “Asian Priorities in Materials Development”, 7–9 June 1999, Novosibirsk, p. 65.

13 K. Heide, Dynamische thermische analysen methoden, Leipzig, 1979, 313 S.

14 V. N. Mitkin, I. M. Oglezneva, *ZhPKh*, 73, 10 (2000) 1595.

15 V. M. Grankin, P. P. Semyannikov, *PTE*, 4 (1991) 129.

16 V. N. Mitkin, P. P. Semjannikov, V. M. Grankin, Third APAM Topical Seminar “Asian Priorities in Materials Development”, 7–9 June 1999, Novosibirsk, p. 58.

17 A. B. Fenelonov, Poristy uglyerod, izd. IK SO RAN, Novosibirsk, 1998.

18 V. N. Mitkin, P. P. Semjannikov, V. M. Grankin, Third APAM Topical Seminar “Asian Priorities in Materials Development”, 7–9 June 1999, Novosibirsk, p. 56.

19 V. N. Mitkin, L. L. Gornostaev, S. V. Filatov *et al.*, Tez. dokl. 1 Vsesoyuz. soveshch. “Litiyevye istochniki toka”, Novocherkassk, 1990, p. 109; V. N. Mitkin, L. L. Gornostaev, *Ibid.*, p. 110.

20 V. N. Mitkin, P. P. Semyannikov, A. A. Galitsky, *Khimiya v interesakh ustoychivogo razvitiya*, 10, 3 (2002) 347.

21 V. V. Malakhov, *J. Mol. Catal.*, A, 158 (2000) 143.

22 L. G. Bulusheva, A. V. Okotrub, V. N. Mitkin *et al.*, *ZhSKh*, 37, 6 (1996) 1072.

23 I. P. Asanov, V. N. Mitkin, L. N. Mazalov, 11th Eur. Symp. on Fluorine Chemistry, 15–22 September 1995, Bled, Slovenia, p. 126.

24 V. N. Mitkin, N. F. Yudanov, A. A. Galitsky *et al.*, Pat. 2103766 RF, 1998.

25 V. N. Mitkin, P. S. Galkin, T. N. Denisova *et al.*, Materials for Electrochemical Energy Storage and Conversion II – Batteries, Capacitors and Fuel Cells, MRS Symp. Proc., vol. 496, Boston, 1998, pp. 57–62.